On the use of a depth-dependent barotropic mode in ocean models: impact on the stability of the coupled barotropic/baroclinic system

Jérémie Demange, Laurent Debreu, Patrick Marchesiello, Florian Lemarié, Eric Blayo

On the use of a depth-dependent barotropic mode in ocean models: impact on the stability of the coupled barotropic/baroclinic system

J. Demange, L. Debreu, P. Marchesiello, F. Lemarié, E. Blayo

RESEARCH REPORT
N° 8589
August 2014
Project-Team MOISE

ISSN 0249-6399 ISRN INRIA/RR--8589--FR+ENG

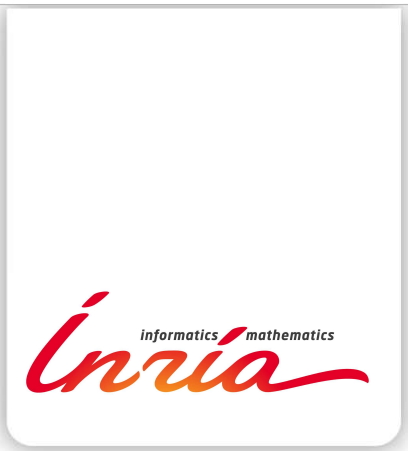

On the use of a depth-dependent barotropic mode in ocean models: impact on the stability of the coupled barotropic/baroclinic system

J. Demange, L. Debreu, P. Marchesiello, F. Lemarié, E. Blayo

Project-Team MOISE

Research Report n° 8589 — August 2014 — 27 pages

Abstract: Evolution of the oceanic free-surface is responsible for the propagation of fast surface gravity waves which roughly propagates at speed $\sqrt{gH}$ (with g the gravity and H the local water depth). In the deep ocean, this phase speed is roughly two orders of magnitude faster than the fastest internal gravity waves. The steep stability constraint imposed by those fast surface waves on the time-step of numerical models is handled using a splitting between slow (internal / baroclinic) and fast (external / barotropic) motions to allow the possibility to adopt specific numerical treatments in each component. The barotropic mode is traditionally approximated by the vertically integrated flow because it has only slight vertical variations. However, the implications of this assumption on the stability of the splitting are not well documented. In this paper, we describe a stability analysis of the mode-splitting technique based on an eigenvector decomposition using the true (depth-dependent) barotropic mode. We show that the use of such a depth-dependent barotropic mode allows a much stable integration of the mode-split equations. As a consequence, the amount of dissipation required to achieve stable integrations, usually applied through averaging filters, can be drastically reduced. It results in a much improved effective resolution even for complex flows. In addition, the formulation of a new mode splitting algorithm using the depth-dependent barotropic mode is introduced. The benefits of this new formulation are illustrated by idealized numerical experiments.

Key-words: Mode splitting, Barotropic mode, Stability analysis

RESEARCH CENTRE
GRENOBLE – RHÔNE-ALPES

Inovallée
655 avenue de l'Europe Montbonnot
38334 Saint Ismier Cedex

Sur l'utilisation d'un mode barotrope dépendant de la profondeur dans les modèles d'océan: impact sur la stabilité du système couplé barotrope/barocline

Résumé : Des déplacements de la surface libre de l'océan résulte la propagation d'ondes de gravité rapides qui se propagent à une vitesse de l'ordre de $\sqrt{gH}$ (avec g la gravité et H la hauteur d'eau locale). Là où l'océan est profond, cette vitesse de phase est environ 2 ordres de grandeur plus rapide que l'onde interne de gravité la plus rapide. La forte contrainte de stabilité imposée par ces ondes rapides de surface sur le pas de temps des modèles est traitée en exploitant une séparation d'échelles entre les mouvements lents (i.e. le mode barocline/interne) et rapides (i.e. le mode barotrope/externe) afin de permettre l'utilisation de schémas numériques adaptés à chaque composante. Le mode barotrope est traditionnellement approché par l'intégrale sur la profondeur de l'écoulement car ses variations sur la verticale sont généralement faibles. Cependant, les conséquences de cette hypothèse sur la stabilité de la séparation d'échelles ont été très peu étudiées jusqu'à maintenant. Dans ce papier, nous développons une analyse de stabilité de la technique de séparation d'échelles en nous basant sur une décomposition en vecteurs propres exhibant le "vrai" mode barotrope (i.e. qui varie avec la profondeur). Nous montrons que l'utilisation de ce mode barotrope dépendant de la profondeur permet une intégration beaucoup plus stable du système couplé barotrope/barocline. Par conséquent, la quantité de dissipation habituellement requise pour stabiliser cette intégration (via des filtres de moyennage) peut être drastiquement réduite. De plus, la formulation d'un nouvel algorithme de séparation d'échelles faisant intervenir un mode barotrope dépendant de la profondeur est introduit. Les avantages de cette nouvelle formulation sont illustrés à l'aide d'expériences numériques.

Mots-clés : Séparation d'échelles, mode barotrope, analyse de stabilité

1 Introduction

Most of the current ocean circulation models have now relaxed the rigid lid assumption and directly integrate a prognostic equation for the free surface evolution. In this case, external gravity waves which roughly propagate at speed $\sqrt{gH}$ (with g the gravity and H the water depth) are explicitly resolved. Because a tridimensional implicit time stepping algorithm seems computationally impractical, the numerical integration of the gravest external waves introduces a strong stability constraint on the model time step. Under several assumptions (including flat bottom), the linear stratified primitive equations can be projected onto a set of normal modes which leads to an orthogonal separation of the modes. This highlights a fast (barotropic) mode and slow (baroclinic) modes. The usual approach in state-of-the-art oceanic models is to introduce a mode splitting where the barotropic mode is integrated separately from the baroclinic modes. In order to satisfy the stability condition, the barotropic part can be integrated using either a 2D implicit time stepping algorithm [6] or a time splitting approach [12]. The use of an implicit algorithm has several drawbacks in particular in term of accuracy (large dispersive errors) and performance on parallel computers, especially at high resolution (poor scaling properties). As a consequence, most of the current ocean models use a time splitting approach where the barotropic component is integrated with several small time steps within a larger baroclinic time step ([2],[12]). In this context, the usual assumption is to consider that the external mode is vertically constant (i.e. depth independent). However, as pointed out in [12], the density field has a nonzero barotropic component which invalidates the depth independent assumption. Although depth-averaging provides an approximation to the barotropic mode , this approximation leads to a non orthogonal separation of slow and fast modes, even in the linear case. A reconciliation of the estimates of the barotropic mode coming from the 2D and the 3D parts is thus needed, and stability of the split between fast and slow modes is not guaranteed (indeed, vertical averaging does not exactly separate out the fast and slow dynamics).

To be more specific, let us introduce the 2D barotropic system linearized around a state of rest

$$\left\{ \begin{array}{rcl} \dfrac{\partial \overline{u}}{\partial t} + g\dfrac{\partial \eta}{\partial x} & = & -\dfrac{1}{\rho_0}\dfrac{\partial}{\partial x}\dfrac{1}{H}\displaystyle\int_{-H}^{0} p_h \mathrm{d}z \\ \dfrac{\partial \eta}{\partial t} + \dfrac{\partial H\overline{u}}{\partial x} & = & 0 \end{array} \right. \tag{1}$$

where $\bar{u}$ is the depth average flow, η the free surface, and the right hand side is the depth integrated internal pressure gradient. This last term is held constant during barotropic integration because the associated purely barotropic component is expected to be rather small. However, we argue that this term is the main source of instability of the splitting under the depth-independent assumption.

To prevent instabilities associated to these splitting errors, a time filtering of the barotropic variables has to be applied. This can be achieved either by using a diffusive time stepping algorithm in the barotropic integration itself [12] or in the baroclinic integration ([8]). This time-filtering is usually done using explicit averaging filters ([16],[18]) applied to the barotropic solution at all subtime steps. In addition to the inexact splitting above, several other reasons motivate the need for some form of time filtering [17, 18]. First, in the nonlinear case, the right hand side of (1) is integrated from $-H$ to η. Because the free surface η itself evolves during the barotropic subtime steps, the consistency is not maintained. An efficient remedy based on a redefinition of the barotropic pressure-gradient terms to account for the local variations in density field is proposed in [17]. Second, aliasing errors due to nonlinearities (when an integral of the advection terms $u \cdot \nabla u$ is also included in (1)) are an additional source of instability controlled by time averaging . The benefit effect of recomputing at least the fast part of this term has been

studied in [15].

The paper deals with the impact of the aforementioned inexact splitting on the stability of numerical models. In [8, 9, 11] , detailed numerical analysis of various 2D/3D time stepping algorithms are presented. Those studies specifically looked at the impact of adding diffusion either in the 2D or in the 3D part of a numerical model. In the present work, the focus is also on the quantification of the impact of the depth-independent assumption on stability of the mode-splitting procedure. Indeed, among aliasing errors, enforcement of 2D/3D consistency, and the inexact splitting, it is yet not well understood which source of error is the most damaging for stability (and consequently which one of those errors justifies the amount of extra diffusion put through time-filtering). An other objective is to provide a general framework for the stability analysis of the mode splitting approach. Unlike previous studies, our analysis is based on a projection of the solution on the basis formed by unapproximated (depth dependent) barotropic and baroclinic modes.

The analysis done here leads to a simple expression of the minimum amount of dissipation required to achieve a stable integration of the mode-split equations. We show that usual explicit averaging filtering techniques are responsible for a much larger dissipation than needed for stability reasons.

The paper is organized as follows. In a first section, we briefly recall the classical theory of vertical mode decomposition and introduce important parameters for the stability analysis. We then proceed to the stability analysis focusing on the amount of diffusion required to control the instability arising from the depth independent barotropic mode assumption. Idealized numerical experiments are performed and the implementation of an alternative splitting technique based on the depth-dependent barotropic mode is introduced.

2 Normal mode decomposition

First, we briefly recall the normal mode decomposition theory (e.g [13, 3]). We consider a linearization of the 2D (x-z) primitive (i.e. under the hydrostatic and Boussinesq assumptions) equations around a motionless state in hydrostatic equilibrium

$$\frac{\partial u}{\partial t} + \frac{1}{\rho_0}\frac{\partial p}{\partial x} = 0 \tag{2}$$

$$\frac{\partial p}{\partial z} = -g\rho \tag{3}$$

$$\frac{\partial u}{\partial x} + \frac{\partial w}{\partial z} = 0 \tag{4}$$

$$\frac{\partial \rho}{\partial t} + w\frac{\mathrm{d}\overline{\rho}}{\mathrm{d}z} = 0 \tag{5}$$

In the vertical direction the model extends from the flat bottom $z = -H$ to the top given by the free surface elevation $z = \eta(x,t)$. Here $u(x,z,t)$ and $w(x,z,t)$ denote the perturbation components of horizontal and vertical fluid velocities (primes are omitted for clarity). $p(x,z,t)$ and $\rho(x,z,t)$ denotes pressure and density perturbations around a state $(\bar{p}(z), \bar{\rho}(z))$ satisfying the hydrostatic relation $\dfrac{\mathrm{d}\bar{p}(z)}{\mathrm{d}z} = -\bar{\rho}(z)g$ where $\overline{\rho}(z)$ is a reference density profile.

The (linearized) surface and bottom boundary conditions read

$$\frac{\partial \eta}{\partial t} = w(z=0) \qquad \text{at } z=0 \tag{6}$$

$$w = 0 \qquad \text{at } z=-H \tag{7}$$

On a vertical grid with n layers, we assume that the discrete solution of (2-5) can be decomposed using vertical modes $M_q(z)$ ([3])

$$u(x,z,t) = \sum_{q=0}^{n-1} u_q(x,t) M_q(z) \tag{8}$$

$$p(x,z,t) = \rho_0 g \sum_{q=0}^{n-1} h_q(x,t) M_q(z) \tag{9}$$

$$\rho(x,z,t) = -\rho_0 \sum_{q=0}^{n-1} h_q(x,t) \frac{\mathrm{d}M_q(z)}{\mathrm{d}z} \tag{10}$$

where the modes $M_q(z)$ are the eigenvectors of the following Sturm Liouville problem

$$\Lambda M_q = \lambda_q M_q \tag{11}$$

$$\left.\frac{\mathrm{d}M_q}{\mathrm{d}z}\right|_{z=-H} = 0 \tag{12}$$

$$\left.\frac{\mathrm{d}M_q}{\mathrm{d}z}\right|_{z=0} = -\frac{N^2(0)}{g} M_q(0) \tag{13}$$

where $\Lambda = -\frac{\mathrm{d}}{\mathrm{d}z}\left(N^{-2}\frac{\mathrm{d}}{\mathrm{d}z}\right)$, with $N^2(z) = -\frac{g}{\rho_0}\frac{\mathrm{d}\overline{\rho}}{\mathrm{d}z}$ the Brünt-Vaisala frequency assumed to be positive. Because Λ is a compact symmetric operator, it admits a basis of orthonormal eigenvectors $M_q(z)$ with positive eigenvalues λ_q. The vertical modes are orthonormal with respect to the dot product $\langle f, g\rangle = \frac{1}{H}\int_{-H}^{0} f(z)g(z)dz$ (the vertical integration extends from $-H$ to 0 instead of η in this linear framework), so that we can write $u_q =< u, M_q >$, and $h_q = \frac{1}{\rho_0 g} < p, M_q >$. The time evolution of u_q and h_q can be obtained as follows:

- (2) is multiplied by $M_q(z)$ and vertically integrated over $[-H, 0]$ (i.e. by taking the dot product) to obtain the time evolution of u_q

$$\frac{\partial u_q}{\partial t} + g\frac{\partial h_q}{\partial x} = 0$$

- (3) is multiplied by $N^{-2}(z)\frac{\mathrm{d}M_q(z)}{\mathrm{d}z}$ and vertically integrated over $[-H, 0]$. The result is integrated by part using (11) and the continuity equation (4) is used to replace the vertical derivatives of w by the horizontal derivative of u. This leads to the time evolution of h_q

$$\frac{\partial h_q}{\partial t} + \frac{1}{g\lambda_q}\frac{\partial u_q}{\partial x} = 0$$

We thus get a set of n uncoupled systems for $0 \leq q \leq n-1$:

$$\frac{\partial u_q}{\partial t} + g\frac{\partial h_q}{\partial x} = 0 \tag{14}$$

$$\frac{\partial h_q}{\partial t} + \frac{1}{g\lambda_q}\frac{\partial u_q}{\partial x} = 0 \tag{15}$$

This can also be expressed in terms of the characteristic variables $y_q^{\pm} = u_q \pm \frac{g}{c_q} h_q$, with $c_q = \sqrt{\frac{1}{\lambda_q}}$, which leads to n transport equations

$$\frac{\partial y_q}{\partial t} \pm c_q \frac{\partial y_q}{\partial x} = 0$$

The c_q term corresponds to the phase speed associated to vertical mode M_q (in particular, c_0 is the speed of external gravity waves).

2.1 Linear stratification case (i.e. $N = cste$)

In this paragraph, we consider the particular case of a constant background stratification N. This simplified case will be useful for the stability analysis presented in Sec. (3.2.1). Let us introduce the dimensionless parameter $\epsilon = N^2 H/g$ whose typical value is such that $\epsilon \ll 1$ (Boussinesq approximation). Indeed , for $N = 10^{-3}\mathrm{s}^{-1}$ and $H = 4000$ m, we get $\epsilon \approx 4.10^{-4}$. The normal mode definition (11-13) can be expressed in terms of ϵ (considering $\lambda_q = c_q^{-2}$)

$$\begin{cases} -\dfrac{\mathrm{d}^2 M_q}{\mathrm{d}z^2} = \epsilon \dfrac{g}{c_q^2 H} M_q \\ \left.\dfrac{\mathrm{d}M_q}{\mathrm{d}z}\right|_{-H} = 0 \\ \left.\dfrac{\mathrm{d}M_q}{\mathrm{d}z}\right|_{0} = -\dfrac{\epsilon}{H} M_q(0) \end{cases} \tag{16}$$

For a constant background stratification, the solution of Sturm-Liouville problem (16) can be found analytically :

$$M_q(z) = M_q(0)\left[\cos\sqrt{\frac{\epsilon g}{c_q^2 H}}z - \sqrt{\frac{\epsilon c_q^2}{gH}}\sin\sqrt{\frac{\epsilon g}{c_q^2 H}}z\right] \tag{17}$$

$$\tan\sqrt{\frac{\epsilon g H}{c_q^2}} = \sqrt{\frac{\epsilon c_q^2}{gH}} \tag{18}$$

The eigenvalues $\lambda_q = c_q^{-2}$ are supposed to be sorted in increasing order. A first approximation of the values of c_q can be obtained by solving (16) with a rigid lid assumption $\left.\dfrac{\mathrm{d}M_q}{\mathrm{d}z}\right|_0 = 0$ for which $\lambda_0 = 0$ (c_0 tends to infinity) and $c_q = \dfrac{NH}{q\pi}$ are small. The knowledge of these orders of magnitude allows now to refine the solutions. The gravest mode (i.e. $q = 0$) is the barotropic

mode for which $\sqrt{\frac{\epsilon g H}{c_0^2}} \ll 1$ since c_0 is large. A Taylor expansion of system (18) in term of ϵ leads at second order to

$$\begin{cases} c_0 = \alpha_0 \sqrt{gH} \text{ with } \alpha_0 = 1 + \frac{\epsilon}{6} - \frac{\epsilon^2}{360} + O(\epsilon^3) \\ M_0(z) = 1 - \epsilon \left[\frac{1}{2} \left(\frac{z}{H} \right)^2 + \frac{z}{H} + \frac{1}{3} \right] + \epsilon^2 \left[\frac{15}{360} \left(\frac{z}{H} \right)^4 + \frac{60}{360} \left(\frac{z}{H} \right)^3 + \frac{120}{360} \left(\frac{z}{H} \right)^2 \frac{120}{360} \left(\frac{z}{H} \right) + \frac{28}{360} \right] + O(\epsilon^3) \end{cases} \tag{19}$$

In particular we have

$$M_0(0) = 1 - \frac{\epsilon}{3} + 7\frac{\epsilon^2}{90}$$

The other eigenvalues (c_q) are obtained by using the fact that c_q are small enough to consider that equation in (18) can be replaced by $\tan \sqrt{\frac{\epsilon g H}{c_q^2}} = 0$. We can find that the baroclinic modes (i.e. for $q \geq 1$) are expressed as:

$$q \geq 1, \quad \begin{cases} c_q = \alpha_q \sqrt{gH} \text{ with } \alpha_q = \frac{\sqrt{\epsilon}}{q\pi} + O(\epsilon^2) \\ M_q(z) = \sqrt{2}[\cos\left(\frac{q\pi}{H} z\right) - \frac{\epsilon}{q\pi} \sin\left(\frac{q\pi}{H} z\right)] + O(\epsilon^2) \end{cases} \tag{20}$$

Figure (1) shows the ratio c_1/c_0 computed from the outputs of a global $1/2^\circ$ simulation using the NEMO ocean model [14]. In agreement with the theory (from (19) and (20) we get $c_1/c_0 \approx \sqrt{N^2 H}/(g\pi)$) its value is small everywhere with the exception of shallow areas where H (hence c_0) decreases.

Note that the stability analysis will essentially use the fact that α_0 is close to 1 but the knowledge of its exact value, obtained here in the case of constant N, is not really required. In the case of non constant N, a good approximation of $c_0^2/(gH)$ has been given in [5] (eq. (29)) for layered ocean models. Under the hydrostatic and Boussinesq assumptions, applying the same technique as in [5] leads to

$$\alpha_0 = \frac{c_0}{\sqrt{gH}} = \sqrt{1 + \frac{1}{gH^2} \int_{-H}^{0} \left(\int_z^0 N^2 (H + z') \mathrm{d}z' \right) \mathrm{d}z}$$

and exactly matches the first order term of our development ($\epsilon/6$) in the case of constant N. In the following we will also use the following equalities (which hold for non constant N):

$$\frac{1}{H} \int_{-H}^{0} M_q(z) \mathrm{d}z = \frac{M_q(0)}{\lambda_q g H} \tag{21}$$

$$\sum_{q=0}^{n-1} \left[\frac{1}{H} \int_{-H}^{0} M_q(z) \mathrm{d}z \right]^2 = 1 \tag{22}$$

The first equality is obtained by vertically integrating the normal mode definition (11) while the second equality is obtained by writing the decomposition of a constant velocity field $u = \sum_{q=0}^{n-1} u_q M_q = 1$ which leads to $u_q =< 1, M_q >= \frac{1}{H} \int_{-H}^{0} M_q(z) \mathrm{d}z$ and $\frac{1}{H} \int_{-H}^{0} u \mathrm{d}z = 1 = \sum_{q=0}^{n-1} \left[\frac{1}{H} \int_{-H}^{0} M_q(z) \mathrm{d}z \right]^2$.

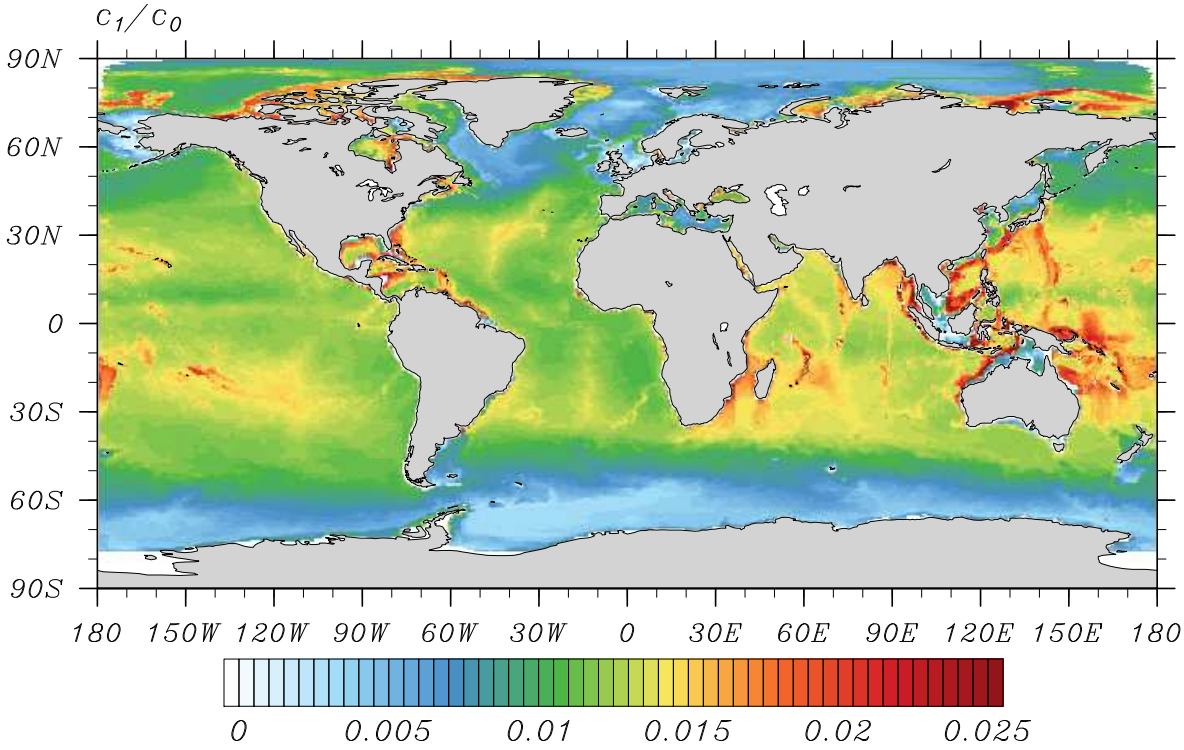

Figure 1: Ratio c_1/c_0 computed from the outputs of a global ORCA 1/2° simulation [14]

2.2 Rigid lid limit

Considering that ϵ is small, the barotropic mode given by (19) can be approximated by $M_0^{\rm rl}(z) = 1$ where the exponent rl stands for rigid lid. It is indeed equivalent to compute the vertical mode assuming a rigid-lid $\dfrac{\partial \eta}{\partial t} = 0$ which results in a modification of the surface boundary condition in $\left.\dfrac{{\rm d}M_0^{\rm rl}(z)}{{\rm d}z}\right|_0 = 0$. Having done this assumption implies a depth independent barotropic mode for which $\dfrac{{\rm d}M_0^{\rm rl}(z)}{{\rm d}z} = 0$. It implies that equation (15) is not valid for $q = 0$ and in addition, instead of (21) we have for $q \geq 1$, we have $\displaystyle\int_{-H}^{0} M_q^{\rm rl}(z) = 0$.

This leads to values of $u_0^{\rm rl}(x,t)$ and $h_0^{\rm rl}(x,t)$ obtained by simple vertical averaging:

$$u_0^{\rm rl}(x,t) = \overline{u}(x,t) = \frac{1}{H}\int_{-H}^{0} u(x,z,t), \quad h_0^{\rm rl}(x,t) = \frac{1}{\rho_0 g}\,\overline{p}(x,t) = \frac{1}{\rho_0 g H}\int_{-H}^{0} p(x,z,t)$$

A direct integration of $h_0^{\rm rl}(x,t)$ is not possible but the pressure can be decomposed in surface and internal values using

$$p(x,z,t) = \rho_0 g\eta + p_h(x,z,t)$$

with

$$p_h(x,z,t) = 0 \tag{23}$$

$$\frac{\partial p_h}{\partial z} = -\rho g \tag{24}$$

so that $h_0^{\rm rl} = \eta + \dfrac{1}{\rho_0 g H}\displaystyle\int_{-H}^{0} p_h$. Time evolution of the free surface η is given by the surface boundary condition (6) :

$$\frac{\partial \eta}{\partial t} = w(z=0)$$

and w at the surface is deduced from the vertical integration of the continuity equation (4) to get $w(x, z=0) = -H\dfrac{\partial \overline{u}}{\partial x}$. The corresponding barotropic system is thus given by:

$$\left\{\begin{array}{rcl} \dfrac{\partial \overline{u}}{\partial t} + g\dfrac{\partial \eta}{\partial x} &=& -\dfrac{1}{\rho_0}\dfrac{\partial}{\partial x}\dfrac{1}{H}\displaystyle\int_{-H}^{0} p_h {\rm d}z \\ \dfrac{\partial \eta}{\partial t} + \dfrac{\partial H\overline{u}}{\partial x} &=& 0 \end{array}\right. \tag{25}$$

The vertically integrated internal pressure gradient evolves slowly in comparison with barotopic variables. While the use of the top boundary condition in the normal mode decomposition leads to n independent shallow water systems of type (14,15), using the rigid lid approximation leads to $n-1$ independent shallow water system of type (14,15) for $q \geq 1$ and the system (25) which actually includes contribution from all the modes. More precisely, the vertical average of internal pressure can be decomposed as

$$\frac{1}{H}\int_{-H}^{0} p_h {\rm d}z = \frac{1}{H}\int_{-H}^{0} \sum_q \rho_0 g h_q \left[M_q(z) - M_q(0)\right] {\rm d}z = \rho_0 g \sum_q \left(\frac{1}{H}\int_{-H}^{0} M_q(z) - M_q(0)\right) h_q \tag{26}$$

The contribution of the barotropic mode is not zero but proportional to $\left(\frac{1}{H}\int_{-H}^{0} M_0(z) - M_0(0)\right)$ which can be expressed at first order in ϵ using (19,21) as

$$\left(\frac{1}{H}\int_{-H}^{0} M_0(z) - M_0(0)\right) = \frac{\epsilon}{3}$$

Maintaining this term constant during the barotropic integration is the main source of instability of the usual mode splitting algorithm.

3 Formulation of the stability analysis using normal mode decomposition

In this section, we explore the stability of the time splitting approach. In order to proceed to the stability analysis of the barotropic/baroclinic mode splitting approach, we will use the basis composed of the rigorous vertical modes $M_q(z)$. Note that expanding the velocity and density fields using the approximated vertical modes $M_q^{\mathrm{rl}}(z)$ is not possible since they do not satisfy the correct surface boundary conditions.

3.1 2D-3D correction

The idea of the mode splitting approach is to integrate separately the 2D and 3D components. When using the rigorous normal mode decomposition, the barotropic component evolves independently of the baroclinic ones so that no correction is needed after the integration of the barotropic system. Contrarily if the depth-independent approximation is made, the 3D system is corrected in order to maintain consistency with the 2D counterpart. An example of a simple time integration algorithm is depicted in figure (2).

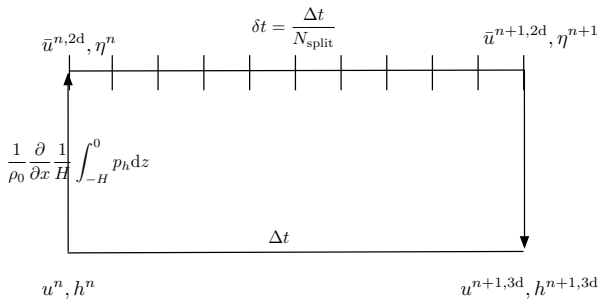

Figure 2: Time splitting algorithm

These corrections are twofold. The first one is to modify the 3D velocities so that their vertical average matches the barotropic velocity. If u^{n+1} and $u^{n+1,\mathrm{c}}$ denotes the 3D velocities at time $n+1$ before and after correction , the correction step reads

$$u^{n+1,\mathrm{c}} = u^{n+1} + \left[\bar{u}^{n+1,2d} - \frac{1}{H}\int_{z}^{0} u^{n+1}\mathrm{d}z\right]$$

In term of projected variables u_q, this correction can be written as

$$u_q^{n+1,c} =< u^{n+1,\mathrm{c}}, M_q >= u_q^{n+1} + \frac{1}{H}\int_{-H}^{0} M_q(z)\mathrm{d}z\left[\bar{u}^{n+1,2d} - \frac{1}{H}\int_z^0 u^{n+1}\mathrm{d}z\right] \tag{27}$$

The second correction is for consistency reason. In the 2D integration, the free surface evolves and this leads to a modification of the surface pressure gradient $p(z=0) = \rho g\eta$. But this evolution has to be in agreement with the modal decomposition which says that $p(z=0) = \rho_0 g \sum_q h_q M_q(0)$.

This second correction has to ensure that

$$p^{n+1}(z=0) = \rho g \eta^{n+1} = \rho_0 g \sum_{q=0}^{n-1} h_q^{n+1} M_q(0) \tag{28}$$

where h_q^{n+1} has evolved through the 3D integration. In the literature this correction is also known as constancy preservation (e.g. [7, 18]). Indeed (28) shows that the density field (hence the h_q components) has to be integrated with a velocity field which has a vertical average that matches the one needed to make the free surface η evolve from n to n+1. In practice two choices are often made. The first option [18] is to integrate the barotropic variables and to deduce a transport which divergence matches the evolution of η from n to $n+1$. This transport is then used to correct (like in eq (27)) the depth average of the 3D velocity that has been used in the integration of the density equation. The second option is to forget the 2D free surface and to recompute it from the 3D velocity fields used to advance the density field. In the next, we will follow the first option. In that case the correction can be written using (22)

$$h_q^{n+1,\mathrm{c}} = h_q^{n+1} + \alpha_q^4 M_q(0)\left(\eta^{n+1,\mathrm{2d}} - \eta^{n+1,\mathrm{3d}}\right), \qquad \text{where } \eta^{n+1,\mathrm{3d}} = \sum_{j=0}^{n-1} h_j^{n+1} M_j(0) \tag{29}$$

Indeed it leads to $\sum h_q^{n+1,\mathrm{c}} M_q(0) = \sum h_q^{n+1} M_q(0) + \left(\eta^{n+1,\mathrm{2d}} - \eta^{n+1,\mathrm{3d}}\right)\sum \alpha_q^4 M_q(0)^2$. Since $\sum \alpha_q^4 M_q(0)^2 = 1$ using (21,22), it shows that $\sum h_q^{n+1,\mathrm{c}} M_q(0) = \eta^{n+1,\mathrm{3d}}$. It is also easy to verify that it exactly corresponds to a correction of the depth average of the 3D velocity that are used to integrate the density field by a two dimensional field $\bar{\bar{u}}$ that satisfies $\dfrac{\eta^{n+1,\mathrm{2d}} - \eta^{n,\mathrm{2d}}}{\Delta t} = -\dfrac{\partial H\bar{\bar{u}}}{\partial x}$. Note that in previous stability analysis found in the literature this correction is not taken into account even if its impact on the stability of the time splitting algorithm is important since the density field has immediately the feedback from the 2D integration.

3.2 Stability analysis using normal mode decomposition

Let $X_q = \begin{pmatrix} u_q \\ h_q \end{pmatrix}$ be the vector of velocity and pressure projections. The system (14,15) can be written as:

$$\frac{\partial X_q}{\partial t} + A_q \frac{\partial X_q}{\partial x} = 0$$

with

$$A_q = \begin{pmatrix} 0 & g \\ \dfrac{c_q^2}{g} & 0 \end{pmatrix}$$

The correction (27,29) is written has:

$$X_q^{n+1,\mathrm{c}} = X_q^{n+1} + C_q \begin{pmatrix} \bar{u}^{n+1,2\mathrm{d}} - \bar{u}^{n+1,3\mathrm{d}} \\ \eta^{n+1,2\mathrm{d}} - \eta^{n+1,3\mathrm{d}} \end{pmatrix} \tag{30}$$

where

$$C_q = \begin{pmatrix} \alpha_q^2 M_q(0) & 0 \\ 0 & \alpha_q^4 M_q(0) \end{pmatrix}$$

The objective is now to express the vector $\begin{pmatrix} \bar{u}^{n+1,2\mathrm{d}} - \bar{u}^{n+1,3\mathrm{d}} \\ \eta^{n+1,2\mathrm{d}} - \eta^{n+1,3\mathrm{d}} \end{pmatrix}$ according to the 2D barotropic integration. The barotropic system (25) can be rewritten as

$$\begin{cases} \dfrac{\partial \overline{u}}{\partial t} + g\dfrac{\partial \zeta}{\partial x} &= 0 \\ \dfrac{\partial \zeta}{\partial t} + \dfrac{\partial H\overline{u}}{\partial x} &= 0 \end{cases} \tag{31}$$

where $\zeta = \eta + \rho_0 g \dfrac{1}{H}\displaystyle\int_{-H}^{0} p_h \mathrm{d}z$ and where we have used the fact that the internal pressure gradient is maintained constant during the barotropic integration. Using $A^{2\mathrm{d}}$ the matrix corresponding to the discrete 2D time stepping algorithm, we write

$$\begin{pmatrix} \bar{u}^{n+1,2d} \\ \zeta^{n+1,2d} \end{pmatrix} = \left[A^{2\mathrm{d}}\right]^{N_{\mathrm{split}}} \begin{pmatrix} \bar{u}^{n} \\ \zeta^{n} \end{pmatrix} \tag{32}$$

where N_{split} is the number of barotropic sub time steps.

The expression in term of evolution of the free surface is thus given by:

$$\begin{pmatrix} \bar{u}^{n+1,2d} \\ \eta^{n+1,2d} \end{pmatrix} = \left[A^{2\mathrm{d}}\right]^{N_{\mathrm{split}}} \begin{pmatrix} \bar{u}^{n} \\ \eta^{n} \end{pmatrix} + \left(\left[A^{2\mathrm{d}}\right]^{N_{\mathrm{split}}} - I\right) \begin{pmatrix} 0 \\ \dfrac{1}{\rho_0 g H}\displaystyle\int_{-H}^{0} p_h \mathrm{d}z \end{pmatrix}$$

The 2D variables $\bar{u}$ and η can be expressed as

$$\bar{u}^{n,3\mathrm{d}} = \sum_q \frac{1}{H}\int_{-H}^{0} M_q(0) u_q^n, \quad \eta^{n,3\mathrm{d}} = \sum_q h_q^n M_q(0)$$

As shown before (26), the decomposition of the internal pressure gradient is:

$$\frac{1}{H}\int_{-H}^{0} p_h \mathrm{d}z = \rho_0 g \sum_q \left(\frac{1}{H}\int_{-H}^{0} M_q(z) - M_q(0)\right) h_q \tag{33}$$

Let us first assume that the internal pressure gradient is computed at time n in (33). In that case we deduce the following expression:

$$\begin{pmatrix} \bar{u}^{n+1,2d} \\ \eta^{n+1,2d} \end{pmatrix} = \sum_i V_i A_i^{2\mathrm{d}} \begin{pmatrix} u_i^n \\ h_i^n \end{pmatrix}$$

with

$$A_i^{2\mathrm{d}} = I + W_i\left(\left[A^{2\mathrm{d}}\right]^{N_{\mathrm{split}}} - I\right), \quad V_i = \begin{pmatrix} \alpha_i^2 M_i(0) & 0 \\ 0 & M_i(0) \end{pmatrix}, \quad W_i = \begin{pmatrix} 1 & 0 \\ 0 & \alpha_i^2 \end{pmatrix}$$

A_i^{2d} is the matrix that makes the projections evolve during the barotropic time step. It is close to $\left[A^{\rm 2d}\right]^{N_{\rm split}}$ for the barotropic component ($i=0$). In the 3D baroclinic time step, we denote by $A_i^{\rm 3d}$ the amplification matrix such that

$$\left(\begin{array}{c} u_i^{n+1,3{\rm d}} \\ h_i^{n+1,3{\rm d}} \end{array}\right) = A_i^{\rm 3d} \left(\begin{array}{c} u_i^{n} \\ h_i^{n} \end{array}\right)$$

so that we deduce that

$$\left(\begin{array}{c} \bar{u}^{n+1,3d} \\ \eta^{n+1,3d} \end{array}\right) = \sum_i V_i A_i^{\rm 3d} \left(\begin{array}{c} u_i^{n} \\ h_i^{n} \end{array}\right)$$

we obtain the relation

$$\left(\begin{array}{c} \bar{u}^{n+1,2d} \\ \eta^{n+1,2d} \end{array}\right) - \left(\begin{array}{c} \bar{u}^{n+1,3d} \\ \eta^{n+1,3d} \end{array}\right) = \sum_i V_i \left(A_i^{\rm 2d} - A_i^{\rm 3d}\right) \left(\begin{array}{c} u_i^{n} \\ h_i^{n} \end{array}\right) \tag{34}$$

Combining (30) and (34), we finally get:

$$\begin{array}{rcl} X_q^{n+1,{\rm corrected}} & = & X_q^{n+1,3{\rm d}} + C_q \sum_i W_i^1 \left(A_i^{\rm 2d} - A_i^{\rm 3d}\right) X_i^{n,3{\rm d}} \\ & = & A_i^{\rm 3d} X_q^{n,3{\rm d}} + C_q \sum_i W_i^1 \left(A_i^{\rm 2d} - A_i^{\rm 3d}\right) X_i^{n,3{\rm d}} \end{array} \tag{35}$$

The main source of instability here is in the evolution of the barotropic components $X_0 = \left(\begin{array}{c} u_0 \\ h_0 \end{array}\right)$ and thus we pay a particular attention on these components in the next paragraph.

3.2.1 Stability via diffusion at the barotropic level

We first study the stability of the 2D integration alone with respect to the barotropic variables (u_0, h_0) and so look at $A_0^{\rm 2d}$. The question is what is the minimum amount of diffusion to add to the 2D integration to compensate the fact that the depth integrated vertical pressure gradient is held constant. Let's suppose that the 2d system (32) has been integrated exactly and integrate a damping factor d_0 (a function of μ_0). In the following, this damping will be put either with an averaging filter or by using a diffusive 2D time stepping. $A^{\rm 2d}$ corresponds to a shallow water system with a propagation speed of $\sqrt{gH}$ (or c_0/α_0) leading to:

$$[A^{\rm 2d}]^{N_{\rm split}} = P_0^{\rm rl} \left(\begin{array}{cc} d_0 e^{-i\mu_0/\alpha_0} & 0 \\ 0 & d_0 e^{i\mu_0/\alpha_0} \end{array}\right) (P_0^{\rm rl})^{-1}, \text{ with } (P_0^{\rm rl})^{-1} = \left(\begin{array}{cc} 1 & \alpha_0 \dfrac{g}{c_0} \\ 1 & -\alpha_0 \dfrac{g}{c_0} \end{array}\right)$$

where $\mu_0 = k c_0 \Delta t$. So that

$$A_0^{\rm 2d} = I + W_0 P_0^{\rm rl} \left(\begin{array}{cc} d_0 e^{-i\mu_0/\alpha_0} - 1 & 0 \\ 0 & d_0 e^{i\mu_0/\alpha_0} - 1 \end{array}\right) (P_0^{\rm rl})^{-1}, \text{ with } W_0 = \left(\begin{array}{cc} 1 & 0 \\ 0 & \alpha_0^2 \end{array}\right)$$

The matrix A_0^{2d} has two complex conjugate eigenvalues and its determinant has the following simple expression :

$$|\lambda_0|^2 = \det(A_0^{2d}) = d_0 \left(\alpha_0^2 d_0 - (\alpha_0^2 - 1)\cos \mu_0/\alpha_0\right) \tag{36}$$

Let us first study low frequencies (or large horizontal scales) $\mu_0 \ll 1$ and assume that at those scales d_0 can be developed as $d_0 = 1 - \gamma\mu_0^2$. A second order Taylor expansion leads to

$$|\lambda_0|^2 = 1 + \left(\frac{1}{2}\frac{\alpha_0^2 - 1}{\alpha_0^2} - \gamma(1+\alpha_0^2)\right)\mu_0^2 \tag{37}$$

Since $\alpha_0 > 1$, this shows that if $\gamma = 0$ (no filtering) the model is unstable at large scales. The minimum value of γ is given by

$$\gamma \geq \frac{\alpha_0^2 - 1}{2\alpha_0^2\,(\alpha_0^2+1)}$$

and (assuming constant N) using expression (19) of α_0 and a first order expansion in ϵ we get:

$$\gamma \geq \frac{\epsilon}{12} \tag{38}$$

(38) is a necessary condition for the stability of the mode splitting approach. It implies that at large scales the filter has to correspond to a second order filter (and not higher order) with a minimum value given by (38).
As can be seen from expression (36), the maximum value of λ_0 are attained at each point where $\cos\mu_0/\alpha_0 = -1$ for which we have $\lambda_0 = d_0\left(\alpha_0^2(d_0+1) - 1\right)$.

Discussion on usual filters and minimal diffusion The preceding results gave us insight on the minimal amount of diffusion that should be present in the 2D step. The objective is now to see if this criterion is full filed by some usual filters. We consider three kinds of filters : two averaging filters with different weights (Flat and Cosine) and a diffusive 2D time stepping. The averaging filters are implemented as

$$\bar{u}^{n+1,2\mathrm{d}} = \sum_{m=0}^{N_{\mathrm{filter}}} a_m u^{m,2\mathrm{d}}$$

where the weights a_m are normalized and such that the average is centered at time $n+1$ (see [17]):

$$\sum_{m=0}^{N_{\mathrm{filter}}} a_m = 1, \quad \sum_{m=0}^{N_{\mathrm{filter}}} a_m \frac{m}{N_{\mathrm{split}}} = 1$$

Note that when using averaging filters, in order to be able to center the average at time $n+1$, the window of integration of the barotropic equations has to extend beyond $n+1$. The expression of the corresponding damping factor d_0 can easily be derived by Fourier transform:

- Flat filter over $n+1-\dfrac{N_{\mathrm{filter}}}{N_{\mathrm{split}}}, n+1+\dfrac{N_{\mathrm{filter}}}{N_{\mathrm{split}}}$, with $N_{\mathrm{filter}} \leq N_{\mathrm{split}}$

$$\begin{aligned} d_0^{\mathrm{Flat}} e^{i\mu_0} = \frac{1}{2N_{\mathrm{filter}}+1} \sum_{m=N_{\mathrm{split}}-N_{\mathrm{filter}}}^{m=N_{\mathrm{split}}+N_{\mathrm{filter}}} e^{im\frac{\mu_0}{N_{\mathrm{split}}}} &= \frac{1}{2N_{\mathrm{filter}}+1}\left[\cos\mu_0\frac{N_{\mathrm{filter}}}{N_{\mathrm{split}}} + \frac{\sin\mu_0\frac{N_{\mathrm{filter}}}{N_{\mathrm{split}}}}{\tan\frac{\mu_0}{2N_{\mathrm{split}}}}\right] e^{i\mu_0} \\ &\approx \frac{\sin\mu_0\frac{N_{\mathrm{filter}}}{N_{\mathrm{split}}}}{\mu_0\frac{N_{\mathrm{filter}}}{N_{\mathrm{split}}}}\, e^{i\mu_0} \text{ for large } N_{\mathrm{split}} \end{aligned}$$

The development of $d_0^{\rm Flat}$ at low frequencies leads to

$$\begin{aligned} d_0^{\rm Flat}(N_{\rm filter}=N_{\rm split}) &= 1-\frac{1}{6}\mu_0^2 \approx 1-0.167\mu_0^2 \\ d_0^{\rm Flat}(N_{\rm filter}=N_{\rm split}/2) &= 1-\frac{1}{24}\mu_0^2 \approx 1-0.042\mu_0^2 \end{aligned} \tag{39}$$

- Cosine filter

$$\begin{aligned} d_0^{\cos}e^{i\mu_0} = \frac{1}{N_{\rm split}}\sum_{m=N_{\rm split}/2}^{m=3N_{\rm split}/2}\left[1+\cos 2\pi\frac{j}{N_{\rm split}}\right]e^{ij\frac{\mu_0}{N_{\rm split}}} &= \frac{2}{N_{\rm split}}\frac{(\sin\frac{\pi}{N_{\rm split}})^2\sin\frac{\mu_0}{2}}{\tan\frac{\mu_0}{2N_{\rm split}}\left(\cos\frac{\mu_0}{N_{\rm split}}-\cos\frac{2\pi}{N_{\rm split}}\right)}e^{i\mu_0} \\ &\approx \frac{\sin(\mu_0/2)}{\frac{\mu_0}{2}(1-\frac{\mu_0^2}{4\pi^2})} \text{ for large } N_{\rm split} \end{aligned}$$

The development of $d_0^{\cos}$ at low frequencies leads to

$$d_0^{\cos} = 1-\left(\frac{1}{24}-\frac{1}{4\pi^2}\right)\mu_0^2 \approx 1-0.016\mu_0^2 \tag{40}$$

- A dissipative Forward backward scheme. Here we don't use an averaging filter but add diffusion inside the 2D time stepping itself.

$$\left\{\begin{array}{rcl} \overline{u}^{n+1} &=& \overline{u}^n - \delta t g\partial_x\eta^n \\ \eta^{n+1} &=& \eta^n - \delta t\partial_x[(1+\theta)\overline{u}^{n+1}-\theta\overline{u}^n]H \end{array}\right. \tag{41}$$

where $\delta t = \dfrac{\Delta t}{N_{\rm split}}$. The corresponding amplification factor over $N_{\rm split}$ time steps writes:

$$d_0^{\rm FB} = \left(\sqrt{1-\theta\left(\frac{\mu_0}{N_{\rm split}}\right)^2}\right)^{N_{\rm split}}$$

The development of d_0 at low frequencies leads to

$$d_0^{\rm FB} = 1-\frac{\theta}{2N_{\rm split}}\mu_0^2$$

So that stability condition (38) requires that

$$\theta \geq \frac{2\epsilon N_{\rm split}}{12} = \frac{\epsilon N_{\rm split}}{6} \tag{42}$$

This shows that the necessary damping increases both when ϵ increases and when the splitting ratio $N_{\rm split}$ increases (knowing that $N_{\rm split}$ is limited by $\dfrac{c_0}{c_1}$).
Note that the stability condition of the Forward Backward scheme (41) requires $(1+\theta)\mu_0 \leq 2$ on a A-grid and $(1+\theta)\mu_0 \leq 1$ on a C-grid.

To illustrate the damping effect of these filters, we fixed some parameters. First we suppose that the 2D integration is integrated with a Courant number equal to CN_0 which leads to $kc_0\delta t = \dfrac{\mu_0}{N_{\rm split}} = \mathrm{CN}_0$. $N_{\rm split}$ has a maximum value which is given by the stability of the first

baroclinic mode. Assuming that the maximum Courant number of the 3D time stepping is 1 ($kc_1\Delta t \leq 1$), this leads to

$$kc_1\Delta t = \mu_0 \frac{c_1}{c_0} \leq 1 \longleftrightarrow N_{\text{split}} \leq \frac{1}{\text{CN}_0}\frac{c_0}{c_1}$$

At first order, the ratio $\dfrac{c_0}{c_1}$ (cf 19,20) is given by $\dfrac{\pi}{N}\sqrt{\dfrac{g}{H}}$. Assuming $\text{CN}_0 = 0.75$, for a value of $H = 4000$m, we study the cases of table (1).

N	$\mu_0 = \dfrac{c_0}{c_1}$	ϵ	$N_{\text{split,max}}$
10^{-2}	15	0.041	20
10^{-3}	155	0.0041	207

Table 1: Set of parameters N and corresponding values of $\mu_0, \epsilon, N_{\text{split,max}}$ for $H = 4000$m

Figure (3) shows the damping factor d_0 for the two averaging filters and for the dissipative Forward Backward scheme. For this last scheme, θ is fixed by the condition (42) for the extreme case of $N = 10^{-2}$ ($\epsilon = 0.041, N_{\text{split,max}} = 20$) which leads to a value of $\theta = \dfrac{\epsilon N_{\text{split,max}}}{6} \approx 0.13$. Two different lengths of the flat weight filter are considered with either $N_{\text{filter}} = N_{\text{split}}$ (in this case the barotropic equations are integrated from t to $t + 2\Delta t$) or $N_{\text{filter}} = \dfrac{N_{\text{split}}}{2}$.

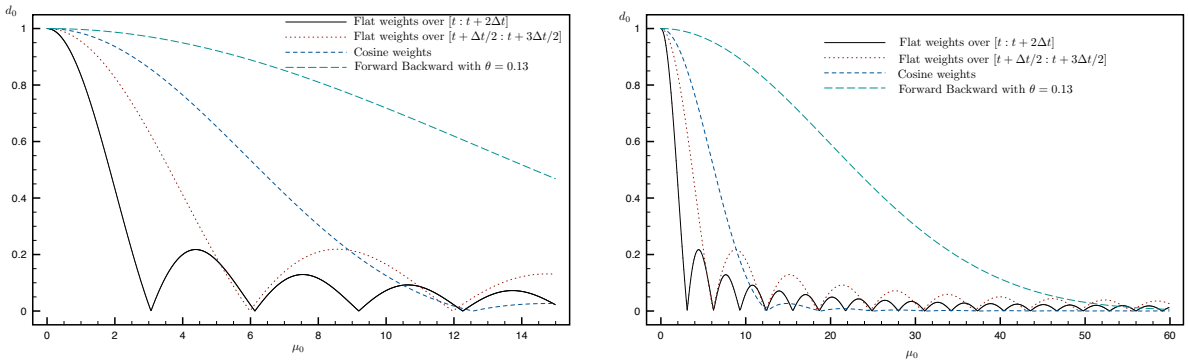

Figure 3: Damping factor as the function of μ_0 for the flat and cosine averaging filters and for the dissipative Forward Backward scheme (with $\theta = 0.13$) for $N = 10^{-2}$ (left), $N = 10^{-3}$ (right)

As expected, the dissipative Forward Backward scheme has much less damping than the averaging filters. Indeed, comparing the developments at large scales of d_0 for the averaging filters (39,40) shows that it is much more than needed by condition (38) which leads to $d_0 = 1 - \dfrac{\epsilon}{6}\mu_0^2 = 1 - \ 0.00683\mu_0^2$ (for the maximum value of $N = 10^{-2}$).

3.2.2 Stability with right hand side extrapolation

In the preceding paragraph, the depth integrated internal pressure gradient was the one computed at time n. There are obviously a lot of other choices (e.g. [17]) than can be studied in the

same framework. Here we look at the possibility of a time extrapolation of this term by using $(1+\beta)h_q^n - \beta h_q^{n-1}$ in (33) (Adams Bashforth like extrapolation). In that case we get, we get

$$\begin{pmatrix} \bar{u}^{n+1,2d} \\ \eta^{n+1,2d} \end{pmatrix} = \sum_i V_i \left[A_i^{2\mathrm{d}} \begin{pmatrix} u_i^n \\ h_i^n \end{pmatrix} + \beta \left(V_i^{-1} \left(\left[A^{\mathrm{fb,2d}} \right]^{N_{\mathrm{split}}} - I \right) W_i^2 \right) \begin{pmatrix} u_i^n - u_i^{n-1} \\ h_i^n - h_i^{n-1} \end{pmatrix} \right] \quad (43)$$

with

$$W_i^2 = \begin{pmatrix} 0 & 0 \\ 0 & (\alpha_i^2 - 1) M_i(0) \end{pmatrix}$$

Looking at the eigenvalues of the $A_0^{2\mathrm{d}}$ matrix and doing a second order Taylor development of its module around $\mu_0 = 0$ leads to

$$|\lambda_0| = 1 - \frac{(3-2\beta)(1-\alpha_0^2) + 2\alpha_0^2(1+\alpha_0^2)\gamma}{4\alpha_0^2}\mu_0^2$$

For $\beta = 1$, we recover the expression (37) and for $\beta = \dfrac{3}{2}$ the scheme is second order accurate at low frequencies.

Now we look at the global spectrum when there is no damping to see the effect of the potential extrapolation ($\beta > 1$). Here we use a perturbation analysis. We inject in the characteristic polynomial of (43) the expression $\lambda_0 = e^{i\mu_0}(1+\xi)$ and solve at first order for ξ (and at first order in ϵ) to find

$$\xi = \frac{1}{6}(1 - e^{i\mu_0})(1 + \beta(-1 + e^{i\mu_0}))\epsilon$$

This leads to a module of the amplification factor equal to:

$$|\lambda_0| = 1 - \frac{1}{3}\left(-1 + 2(-1+\beta)\cos\mu_0\right)\left(\sin\frac{\mu_0}{2}\right)^2 \epsilon$$

For $\beta \geq 1$, maximum values of $|\lambda_0|$ are attained at each point where $\cos\mu_0 = -1$ ($\mu_0 = (2p+1)\pi$ with p an integer). At these points we have:

$$|\lambda_0|_{\max} = 1 + \frac{1}{3}\left(-1 + 2\beta\right)\epsilon$$

and the apparent problem is that this maximum value is increased when β is increased. Figure (4) shows this amplification factor for the case $\epsilon = 0.041$, corresponding to $N = 10^{-2}$ (the exact amplification is not shown since it matches perfectly the approximation).

If filtering is added, the first objective will be to counter the two instabilities seen at large scales (present if $\beta < \dfrac{3}{2}$) and at each aliasing frequency $\mu_0 = (2p+1)\pi$. As before, we now add a damping factor d_0 and compute the module of the eigenvalue at $\mu_0 = \pi$ to get

$$|\lambda_0|_{\max}(\mu_0 = \pi) = d_0 + \frac{1}{3}\left(-1 + 2\beta\right)\epsilon \quad (44)$$

We now consider the possibility of adding second or fourth order diffusion to the 2D integration.

- Second order diffusion. Let's suppose we use a second order filter and express d_0 at second order in μ_0[1] as $d_0 = 1 - \gamma\mu_0^2$. The condition at $|\lambda_0|_{\max}(\mu_0 = \pi) \leq 1$ writes:

$$\gamma \geq \frac{1}{\pi^2}\frac{1}{3}\left(-1 + 2\beta\right)\epsilon$$

[1]Here we assume that the additional filtering is achieved through a 2D dissipative time filter. Obviously μ_0 is not small at the value we are interested in ($\mu_0 = \pi$) but the Taylor development is actually done in term of μ_0/N_{split}

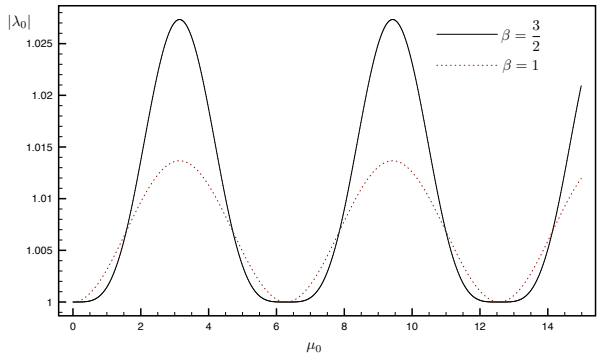

Figure 4: Amplification factor of the barotropic mode $|\lambda_0|$ without ($\beta = 1$) and with ($\beta = \frac{3}{2}$) right hand side extrapolation

For $\beta = 1$ (no right hand side extrapolation) it leads to $\gamma \geq \frac{\epsilon}{3\pi^2}$ with is less restrictive than the condition at large scales (38) $\gamma \geq \frac{\epsilon}{12}$.
For $\beta = \frac{3}{2}$, there is no instability at large scales and the previous condition leads to:

$$\gamma \geq \frac{2}{3\pi^2}\epsilon$$

which is (only) slightly less restrictive that condition (38). The right hand side extrapolation allows to be second order accurate at large scales but does not really reduce the amount of required damping.

- Fourth order diffusion. Let's assume now that right hand side extrapolation has been done ($\beta \geq \frac{3}{2}$) so that second order diffusion at large scales is not required. Thus we can also try to apply fourth order diffusion with $d_0 = 1 - \gamma_4 \mu_0^4$ and the condition $|\lambda_0|_{\max}(\mu_0 = \pi) \leq 1$ leads to:

$$\gamma_4 \geq \frac{1}{\pi^4}\frac{1}{3}\left(-1 + 2\beta\right)\epsilon$$

which give for $\beta = 3/2$

$$\gamma_4 \geq \frac{2}{3\pi^4}\epsilon \tag{45}$$

This is however a rather large biharmonic diffusion coefficient. Indeed if view in term of added diffusion in the 2D time stepping:

$$d_0 = \left[1 - \gamma_{2\mathrm{d}}\left(\frac{\mu_0}{N_{\mathrm{split}}\alpha_0}\right)^4\right]^{N_{\mathrm{split}}}$$

Developing for μ_0 small, leads to

$$d_0 = 1 - \frac{\gamma_4}{N_{\mathrm{split}}^3}\mu_0^4 \tag{46}$$

so that (45) is satisfy if

$$\gamma_{2\mathrm{d}} \geq \frac{2}{3\pi^4}\epsilon N_{\mathrm{split}}^3$$

For the extreme case used abose of $\epsilon = 0.041, N_{\mathrm{split}} = 20$ this gives $\gamma_{2\mathrm{d}} \geq 2.2$. This large value of biharmonic diffusion would severely constrain the time step of the barotropic integration.

3.2.3 Addition of the first baroclinic mode

We here add one baroclinic mode in the analysis, mainly to look at the damping of the first baroclinic mode associated with the 2D filtering. We assume no right hand side extrapolation $\beta = 1$. The system coming from (35) can be written as :

$$\left((X_q)^{n+1,\mathrm{corrected}}\right)_{q=1,2} = G\left((X_q)^n\right)_{q=1,2}$$

with

$$G = \begin{pmatrix} C_0 W_0^1 A_0^{2\mathrm{d}} + \left(I - C_0 W_0^1\right) A_0^{3d} & C_0 W_1^1 \left(A_1^{2\mathrm{d}} - A_1^{3\mathrm{d}}\right) \\ C_1 W_0^1 \left(A_0^{2\mathrm{d}} - A_0^{3\mathrm{d}}\right) & A_1^{3\mathrm{d}} + C_1 W_1^1 \left(A_1^{2\mathrm{d}} - A_1^{3\mathrm{d}}\right) \end{pmatrix}$$

The amplifications of the barotropic and baroclinic mode are plotted on figures (5,6,7). Note that at the difference to the preceding plots, here the amplification is plotted against an inverse horizontale scale $k\Delta x = \mu_0/(N_{\mathrm{split}}\mathrm{CN}_0)$. Figure (5) shows the amplifications without any filtering. The barotropic mode is unstable at all scales while the baroclinic modes have small instabilities at small scales [2].

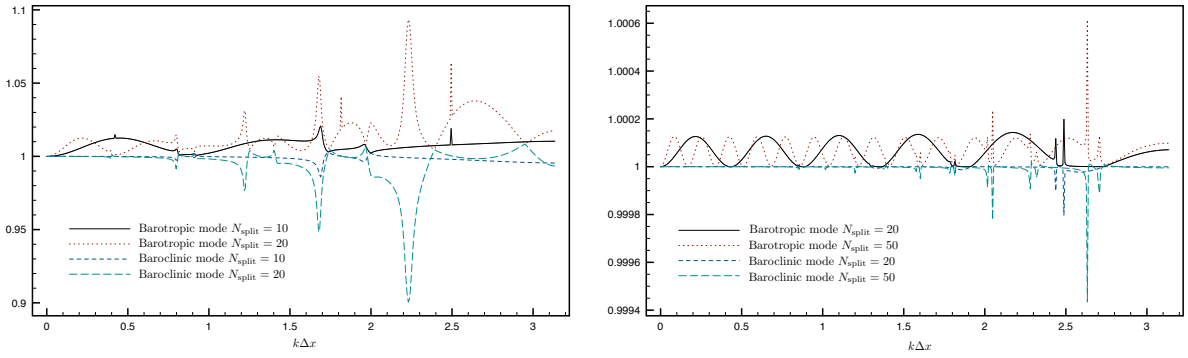

Figure 5: Barotropic and first baroclinic mode amplification without filtering for different splitting ratio N_{split}. $N = 10^{-2}$ left, $N = 10^{-3}$ right

Figure (6) (resp. (7)) shows the same amplifications factor with added filtering for the case $N = 10^{-2}$ (resp. $(N = 10^{-3})$). The filtering is added either using a flat weight filter (over $t, t + 2\Delta t$) or using a 2D Forward backward diffusive time stepping (with $\theta = 0.13$ as above). All filters are able to stabilize the integration and as expected the dissipative Forward Backward scheme is less diffusive than the averaging filters.

[2] This last point can also easily be derived by building the matrix G_{char} of evolution of the characteristics variables $Y_q = \begin{pmatrix} y_q^+ \\ y_q^- \end{pmatrix}$ and computing the eigenvalues of G_{char} as perturbations of a diagonal matrix with exact amplification factors $\mathrm{Diag}[(e^{i\mu_0}, e^{-i\mu_0}, e^{i\mu_1}, e^{-i\mu_1})]$ with $\mu_1 = kc_1\Delta t$

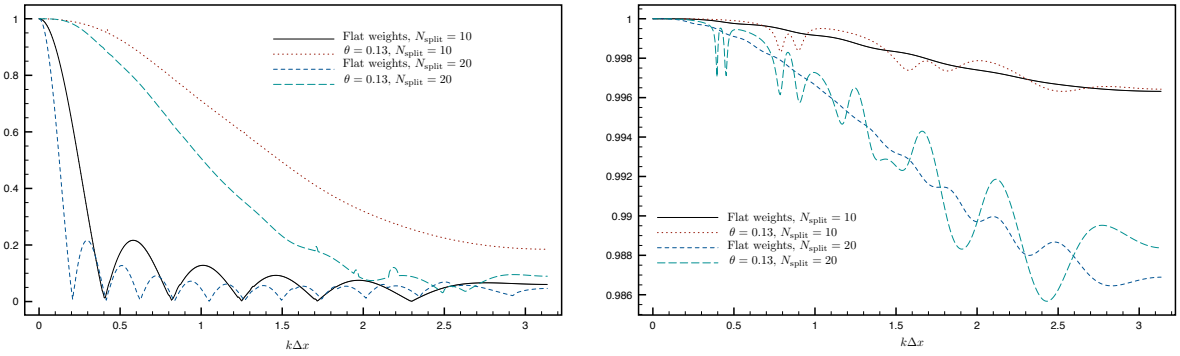

Figure 6: Barotropic (left) and first baroclinic mode (right) amplification with different filters and different splitting ratio N_{split} for $N = 10^{-2}$

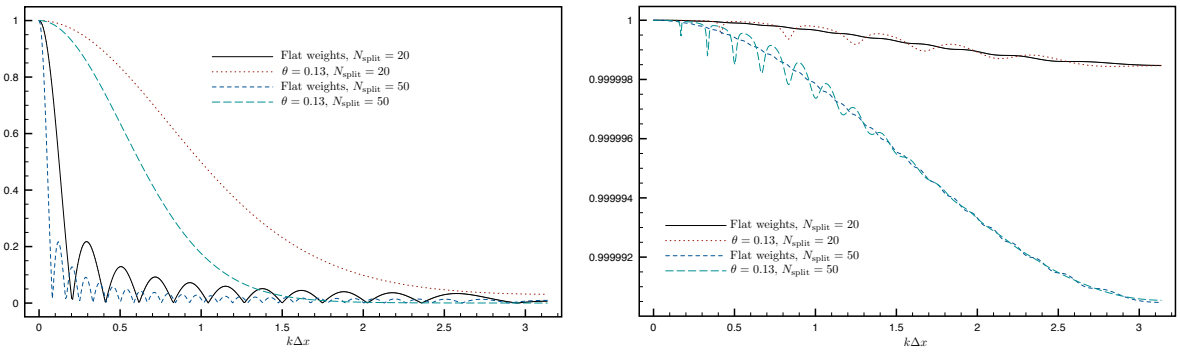

Figure 7: Barotropic (left) and first baroclinic mode (right) amplification with different filters and different splitting ratio N_{split} for $N = 10^{-3}$

3.3 Partial conclusions

The stability analysis has first confirm that the source of instability of the inexact splitting comes from the fast part of the depth integrated internal pressure gradient that is held constant during the barotropic integration. The time extrapolation of the right hand side enables to be second order at large scales for the barotropic mode but does not improve the stability. In this stability analysis framework, it is naturally sufficient to study the evolution of the (true) barotropic mode since the other baroclinic mode require much less damping.

4 Numerical implementation of a barotropic/baroclinic mode splitting and idealized test case

In this section, we will illustrate the theoretical study on a simple idealized test case that rely on the linearized (around a state at rest) primitive equations (2,3,4,5). We also formulate a splitting based on the use of the true depth-dependent barotropic mode. We begin by its practical implementation then show how the barotropic corrections are handled and finally show the results

of the numerical experiments.

4.1 Practical implemtation of the (depth-dependent) barotropic/baroclinic mode splitting

The integration of the barotropic part is given by eqs (14,15) for $q = 0$

$$\frac{\partial u_0}{\partial t} + g\frac{\partial h_0}{\partial x} = 0, \quad \frac{\partial h_0}{\partial t} + \frac{c_0^2}{g}\frac{\partial u_0}{\partial x} = 0 \tag{47}$$

For the practical implementation, we reformulate this equation in term of u_0, η, ρ_b where

$$\rho_b = \frac{1}{H}\int_{-H}^{0} \rho(x,z,t)N^{-2}(z)\frac{\mathrm{d}M_0(z)}{\mathrm{d}z}\mathrm{d}z$$

ρ_b is the barotropic component of the density field and is zero when the barotropic mode is assumed to be depth-independent. One of the reason of introducing ρ_b and η is to able to have access to the free surface elevation during the barotropic integration. It may be useful for example if the free surface is used in the boundary conditions. But there is a more fundamental reason. If h_0 is computed inside the barotropic integration, then at the end of this integration the correction naturally apply to the barotropic component of the pressure field. However when discretized on a vertical Lorenz grid, the presence of a computational mode ([1],[10]) prevents from uniquely deducing from a correction on the pressure field a correction on the density field (that is what is needed at the end).
From the decomposition of ρ (10), we can prove that:

$$h_0 = \frac{M_0(0)}{\lambda_0 g H}\,\eta - \frac{1}{\lambda_0}\,\frac{\rho_b}{\rho_0} \tag{48}$$

Note that is this expression $\dfrac{M_0(0)}{\lambda_0 g H}$ is actually equals to the vertical integral of the barotropic mode $\displaystyle\int_{-H}^{0} M_0(z)\mathrm{d}z$. Integrating (48) in (47) leads to

$$\frac{\partial u_0}{\partial t} + \frac{\partial}{\partial x}\left[\frac{M_0(0)}{\lambda_0 H}\,\eta - \frac{g}{\lambda_0\rho_0}\,\rho_b\right] = 0, \quad \frac{\partial \rho_b}{\partial t} - \frac{\rho_0 M_0(0)}{gH}\frac{\partial \eta}{\partial t} - \frac{\rho_0}{g}\frac{\partial u_0}{\partial x} = 0$$

The time evolution of η is as usual given by the free surface condition:

$$\frac{\partial \eta}{\partial t} + \frac{\partial H\bar{u}}{\partial x} = 0$$

where $\bar{u}$ is expressed as a function of u_0 and the truly baroclinic part:

$$\bar{u}(x,t) = \frac{1}{H}\int_{-H}^{0} u(x,z,t) = \frac{1}{H}\int_{-H}^{0}[u_0(x,t)M_0(z) + u'(x,z,t)] = \frac{M_0(0)}{\lambda_0 g H}\,u_0(x,t) + \frac{1}{H}\int_{-H}^{0} u'(x,z,t)$$

$\dfrac{1}{H}\displaystyle\int_{-H}^{0} u'(x,z,t)$ contains only baroclinic modes and thus is the slow part of the depth averaged velocity. In practice, this term is computed at the beginning of the barotropic integration and

is held constant over the barotropic time steps (even if it can also be extrapolated). The final form of the barotropic equations is:

$$\left\{\begin{array}{l} \dfrac{\partial u_0}{\partial t} + \dfrac{\partial}{\partial x}\left[\dfrac{M_0(0)}{\lambda_0 H}\,\eta - \dfrac{g}{\lambda_0\rho_0}\,\rho_b\right] = 0 \\ \dfrac{\partial \rho_b}{\partial t} + \dfrac{\rho_0 M_0(0)}{gH}\dfrac{\partial H\bar{u}}{\partial x} - \dfrac{\rho_0}{g}\dfrac{\partial u_0}{\partial x} = 0 \\ \bar{u} = \dfrac{M_0(0)}{\lambda_0 gH}\,u_0 + \dfrac{1}{H}\displaystyle\int_{-H}^{0} u'(x,z,t) \\ \dfrac{\partial \eta}{\partial t} + \dfrac{\partial H\bar{u}}{\partial x} = 0 \end{array}\right.$$

and we recall that when a vertically constant barotropic mode is assumed, the barotropic system writes:

$$\left\{\begin{array}{rcl} \dfrac{\partial \bar{u}}{\partial t} + g\dfrac{\partial \eta}{\partial x} & = & -\dfrac{1}{\rho_0}\dfrac{\partial}{\partial x}\dfrac{1}{H}\displaystyle\int_{-H}^{0} p_h dz \\ \dfrac{\partial \bar{\eta}}{\partial t} + \dfrac{\partial H\bar{u}}{\partial x} & = & 0 \end{array}\right.$$

4.2 Correction of 3d variables

The correction step, that makes the barotropic mode coincides with the 3D part has been explained in (3.1) for the case of depth-independent barotropic mode. In the depth-dependent case, it includes in addition a correction of the density field and writes:

$$\left\{\begin{array}{l} \dfrac{1}{H}\displaystyle\int_{-H}^{0} u^{n+1,c} M_0 = u_0^{n+1} \\ \dfrac{1}{H}\displaystyle\int_{-H}^{0} \rho^{n+1,c} N^{-2}\dfrac{\mathrm{d}M_0(z)}{\mathrm{d}z} = \rho_b^{n+1} \\ p^{n+1}(0) = \rho_0 g \eta^{n+1} \end{array}\right.$$

The velocity correction is done as follows

$$u^{n+1,c} = u^{n+1} + \left[u_0^{n+1} - \frac{1}{H}\int_{-H}^{0} u^{n+1} M_0(z)\mathrm{d}z\right] M_0(z)$$

while the density correction is done as follows

$$\rho^{n+1,c} = \rho^{n+1} + \frac{1}{\lambda_0 - \frac{M_0(0)^2}{gH}}\left[\rho_b^{n+1} - \frac{1}{H}\int_{-H}^{0} \rho^{n+1} N^{-2}\frac{\mathrm{d}M_0(z)}{\mathrm{d}z}\right]\frac{\mathrm{d}M_0(z)}{\mathrm{d}z}$$

4.3 Test case

Configuration and model initialization The domain is periodic of size $L_x = 10000$km with a depth of $H = 4$km. The Brünt Vaisala frequency N is taken equal to $10^{-3}\mathrm{s}^{-1}$. The model is initialized with a barotropic solution with a right travelling wave ($y_0^- = u_0 - \dfrac{g}{c_0}h_0 = 0$).

$$h_0(x, t=0) = 10\sin\left(\frac{2\pi}{L_x}x\right)e^{-(x-L_x/2)^2/\Delta^2}, \quad u_0(x,t=0) = \frac{g}{c_0}h_0(x,0)$$

with $\Delta = 2000$km. The velocity, density and free surface are then deduced:

$$u(x,z,t=0) = u_0(x,t=0)M_0(z), \quad \rho(x,z,t=0) = -\rho_0 h_0(x,t=0)\frac{\mathrm{d}M_0(z)}{\mathrm{d}z}, \quad \eta(x,t=0) = h_0(x,t=0)M_0(0)$$

The initial condition $\rho(x,z,t=0)$ is plotted on figure (8):

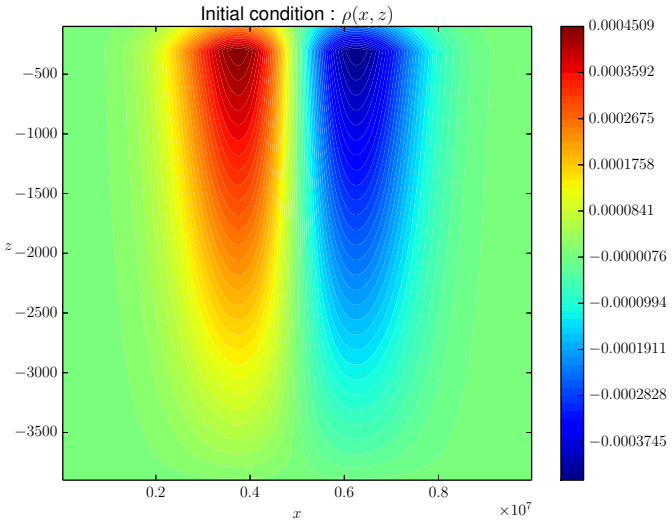

Figure 8: Initial value of the density field

Discretization and numerical schemes The model uses usual horizontal staggered grid and a Lorenz vertical grid with a geopotential vertical coordinates. It uses second order finite differences. The 3D time integration scheme is a non dissipative Euler Forward Backward scheme. The 2D time integration is also based on a (possibly dissipative) Forward Backward scheme. The value of the baroclinic time steps is chosen so that the 2D Courant number $\mathrm{CFL}_{2D} = \dfrac{c_0\Delta t}{\Delta x} = 0.75$. The splitting ratio is taken to $N = 60$ leading to a value of $\mathrm{CFL}_{3D} = \dfrac{c_1\Delta t}{\Delta x} = 0.31$ .The number of horizontal and vertical grid cells are $n_x = 200, n_z = 20$ leading to horizontal and vertical grid resolutions of $\Delta x = 50$km, $\Delta z = 50$m.

Results As a diagnostic of the induced damping of the different filtering techniques we look at the evolution of the maximum of the free surface elevation. Figure (9) shows the results obtained with filtering techniques presented in (3.2.1). In addition to the flat and cosine weights described above, we add results obtained with the second order power law averaging filter implemented in the ROMS ([17]). The reference solution corresponds to a simulation without splitting (the time step is constrained by the barotropic mode). The amount of dissipation vary quite strongly between the different filters and as expected the use of the second order power law filter reduces the damping of the free surface elevation. Of course, without any filtering, the solutions are blowing up quite rapidly.
Figure (10) add two others numerical solutions. The first one corresponds to the use of a diffusive

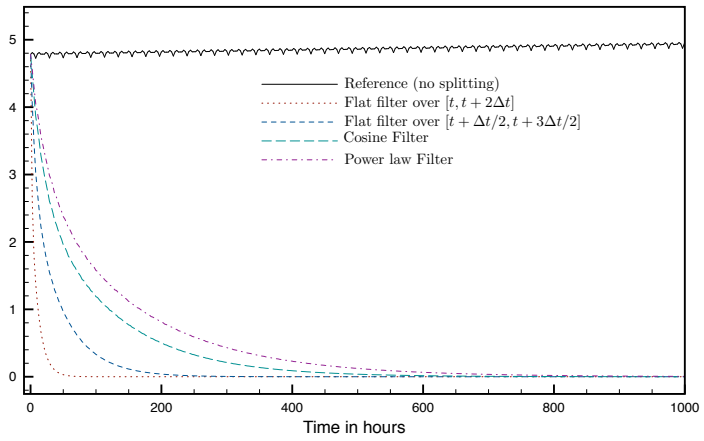

Figure 9: Time evolution of the maximum of the free surface elevation. Comparaison of usual filters against a reference solution without splitting

2D time stepping using a forward backward scheme with $\theta = 0.13$ and the second one is based on the use of the true depth-dependent barotropic mode (see 4.1) without any filtering. The use of a dissipative 2D time stepping is stable and introduces much less damping than the averaging filters. Since there is no damping, the solution obtained with the true barotropic mode, matches exactly the reference solution.

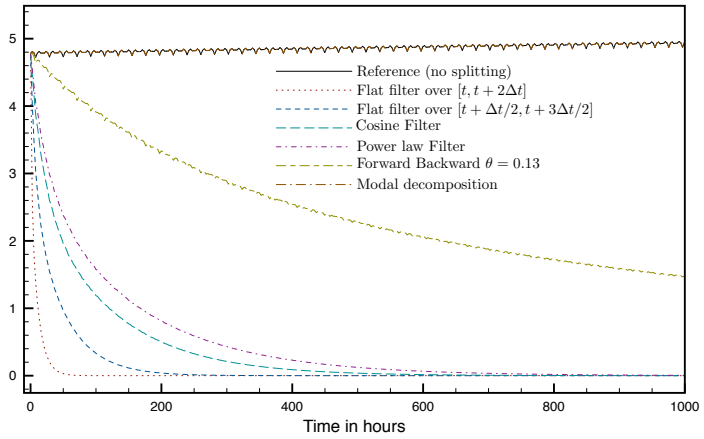

Figure 10: Time evolution of the maximum of the free surface elevation. Comparaison of usual filters against a reference solution without splitting

5 Conclusion

Barotropic/baroclinic mode splitting for free surface ocean models remains an issue to consider since it can require a large amount of unphysical diffusion to achieve a stable integration of the mode-split equations. In this paper, we introduce a framework for the stability analysis of the splitting technique. This is based on a decomposition that uses the true (depth-dependent) barotropic mode as opposed to the traditional depth-independent assumption adopted in realistic oceanic models which require extra sources of diffusion to maintain stability (either through time-filters or dissipative integration schemes). Our study reveals that the amount of diffusion induced by classical averaging filters is much larger than needed to compensante the inexact mode splitting (i.e. under the depth-independent assumption). We thus favor the use of slightly dissipative 2D time stepping algorithms. Moreover, our stability analysis allows to quantify the minimum amount of required diffusion necessary to counteract mode splitting instabilities arising linked with the depth-dependant barotropic mode approximation. The numerical experiments were done here in a very simplified model where all the assumptions of the normal mode decomposition are valid. We have however also run several realistic experiments using the ROMS model. Adding to the 2D barotropic time stepping algorithm an amount of laplacian diffusion corresponding to the theoretical study presented in this paper (and removing the existing averaging filter) has led to long terms stable runs. Using 2D dissipative time stepping algorithms has several additional advantages over the averaging filters. First the barotropic integration stops at time $n + 1$ and does not require additional time steps like in averaging filters. This lowers the computational cost, especially on parallel computers where the 2D integration is the less scalable part of the numerical model. It also allows to obtain a continuous free surface elevation. Finally it strongly simplifies the implementation of grid nesting with coupling at the barotropic level ([4]).

The formulation of a mode splitting technique that uses the depth-dependent barotropic mode has been introduced. In this formulation, the barotropic component of both velocities and density are integrated with small time steps. Several developments are still needed to be able to use this formulation in a realistic context (e.g. non flat bottom) where the normal mode decomposition in not valid and possibly where the density itself is not integrated but diagnosed from temperature and salinity. But the hope is that, even if approximated in this case, this formulation will allow the use of less diffusion than in current ocean models to maintain good stability properties.

Acknowledgements

E. Blayo, J. Demange, L. Debreu, and P. Marchesiello were funded by the ANR through contract ANR-11-MONU-005 (COMODO). F. Lemarié acknowledges the support of the French LEFE MANU and GMMC programs through project CHRONOS.

References

[1] A. Arakawa and C. S. Konor. Vertical differencing of the primitive equations based on the charney-phillips grid in hybrid sigma-p vertical coordinates. Monthly weather review, 124(3):511–528, 1996. eng.

[2] Hans Berntsen, Zygmunt Kowalik, Steinar Sælid, and Karstein Sørli. Efficient numerical simulation of ocean hydrodynamics by a splitting procedure. Modeling, Identification and Control, 2(4):181–199, 1981.

[3] E. Blayo and L. Debreu. Revisiting open boundary conditions from the point of view of characteristic variables. Ocean Modelling, 9(3):231 – 252, 2005.

[4] Laurent Debreu, Patrick Marchesiello, Pierrick Penven, and Gildas Cambon. Two-way nesting in split-explicit ocean models: Algorithms, implementation and validation. Ocean Modelling, 49–50(0):1 – 21, 2012.

[5] John K. Dukowicz. Structure of the barotropic mode in layered ocean models. Ocean Modelling, 11(1–2):49 – 68, 2006.

[6] John K. Dukowicz and Richard D. Smith. Implicit free-surface method for the bryan-cox-semtner ocean model. Journal of Geophysical Research: Oceans, 99(C4):7991–8014, 1994.

[7] Stephen M. Griffies, Ronald C. Pacanowski, Martin Schmidt, and V. Balaji. Tracer conservation with an explicit free surface method for z-coordinate ocean models. Monthly Weather Review, 129(5):1081–1098, 2014/08/12 2001.

[8] Robert Hallberg. Stable split time stepping schemes for large-scale ocean modeling. Journal of Computational Physics, 135(1):54 – 65, 1997.

[9] Robert L. Higdon and Roland A. de Szoeke. Barotropic-baroclinic time splitting for ocean circulation modeling. Journal of Computational Physics, 135(1):30 – 53, 1997.

[10] D. Holdaway, J. Thuburn, and N. Wood. Comparison of lorenz and charney–phillips vertical discretisations for dynamics–boundary layer coupling. part i: Steady states. Quarterly Journal of the Royal Meteorological Society, 139(673):1073–1086, 2013.

[11] V.M. Kamenkovich and D.A. Nechaev. On the time-splitting scheme used in the princeton ocean model. Journal of Computational Physics, 228(8):2874 – 2905, 2009.

[12] Peter D. Killworth, David J. Webb, David Stainforth, and Stephen M. Paterson. The development of a free-surface bryan–cox–semtner ocean model. Journal of Physical Oceanography, 21(9):1333–1348, 2014/07/29 1991.

[13] P. K. Kundu and I. M. Cohen. Fluid Mechanics, Second Edition. Academic Press, 2002.

[14] J. M. Molines, B. Barnier, T. Penduff, L. Brodeau, A.M. Treguier, S. Theetten, and G. Madec. Definition of the global 1/2° experiment with CORE forcing, ORCA05-G50. Technical report, LEGI-DRA-1-11-2006, 2007.

[15] Yves Morel, Remy Baraille, and Annick Pichon. Time splitting and linear stability of the slow part of the barotropic component. Ocean Modelling, 23(3-4):73 – 81, 2008.

[16] B.T. Nadiga, M.W. Hecht, L.G. Margolin, and P.K. Smolarkiewicz. On simulating flows with multiple time scales using a method of averages. Theoretical and Computational Fluid Dynamics, 9(3-4):281–292, 1997.

[17] Alexander F. Shchepetkin and James C. McWilliams. The regional oceanic modeling system (roms): a split-explicit, free-surface, topography-following-coordinate oceanic model. Ocean Modelling, 9(4):347 – 404, 2005.

[18] Alexander F. Shchepetkin and James C. McWilliams. Computational kernel algorithms for fine-scale, multiprocess, longtime oceanic simulations. In P.G. Ciarlet, editor, Handbook of Numerical Analysis, volume 14 of Handbook of Numerical Analysis, pages 121 – 183. Elsevier, 2009.

Contents

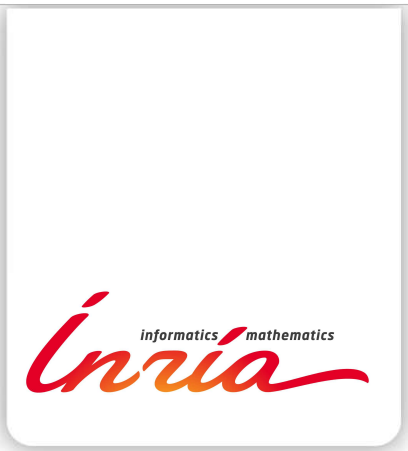

RESEARCH CENTRE
GRENOBLE – RHÔNE-ALPES

Inovallée
655 avenue de l'Europe Montbonnot
38334 Saint Ismier Cedex

Publisher
Inria
Domaine de Voluceau - Rocquencourt
BP 105 - 78153 Le Chesnay Cedex
inria.fr

ISSN 0249-6399